

A study of the freezing transition in the LennardJones system

Biman Bagchi, Charles Cerjan, and Stuart A. Rice

Citation: *The Journal of Chemical Physics* **79**, 6222 (1983); doi: 10.1063/1.445726

View online: <http://dx.doi.org/10.1063/1.445726>

View Table of Contents: <http://scitation.aip.org/content/aip/journal/jcp/79/12?ver=pdfcov>

Published by the AIP Publishing

Articles you may be interested in

[Precise simulation of the freezing transition of supercritical Lennard-Jones](#)

J. Chem. Phys. **135**, 154103 (2011); 10.1063/1.3651193

[Accurate freezing and melting equations for the Lennard-Jones system](#)

J. Chem. Phys. **134**, 094108 (2011); 10.1063/1.3561698

[Reply to the Comment on "Monte Carlo studies of the fluid–solid phase transition in the LennardJones system"](#)

J. Chem. Phys. **62**, 4582 (1975); 10.1063/1.430380

[Freezing and melting properties of the LennardJones system](#)

J. Chem. Phys. **61**, 1970 (1974); 10.1063/1.1682198

[Monte Carlo studies of the fluidsolid phase transition in the LennardJones system](#)

J. Chem. Phys. **61**, 1960 (1974); 10.1063/1.1682197



A study of the freezing transition in the Lennard-Jones system

Biman Bagchi,^{a)} Charles Cerjan,^{b)} and Stuart A. Rice

Department of Chemistry and The James Franck Institute, The University of Chicago, Chicago, Illinois 60637
(Received 1 July 1983; accepted 22 July 1983)

The freezing of a Lennard-Jones fluid into a face-centered-cubic lattice is examined within the framework of a recently proposed analysis of the nonlinear integral equation that relates the densities of the coexisting liquid and solid phases. The temperature dependent densities of the liquid and solid phases along the coexistence line in the temperature-density plane are calculated and found to be in reasonable agreement with the results of computer simulations.

I. INTRODUCTION

In a recent paper¹ we reported a theory of freezing based on analysis of the solutions of the equation describing the inhomogeneous density distribution at phase equilibrium. This analysis takes the form of a search for a bifurcation point where the uniform density characteristic of the fluid phase becomes thermodynamically unstable relative to the periodic density distribution of the crystalline phase. The theory described, as applied to the hard sphere fluid, is an extension of the work of Ryzhov and Tareeva,² and it properly accounts for the jump discontinuity in the density at the liquid-solid transition. If carried through exactly, the bifurcation analysis will locate the true equilibrium transition and not display metastability in either the fluid or solid phases. Of course, as in all other many body theories, it is necessary to make approximations in order to reduce the formally correct equations derived to tractable form. The approximations introduced in our earlier work were: (a) truncation of the exact expansion for the density in an inhomogeneous system at the level of the direct correlation function for pairs of molecules; (b) the use of a convenient but inexact direct correlation function for the liquid; (c) the use of an order parameter expansion which neglects vibrational motion in the solid; and (d) the truncation of the order parameter expansion for the density difference between phases after a few terms. It was shown that, despite these simplifying approximations, the theory successfully predicts the existence of the liquid-solid transition in the hard sphere system and gives moderately good values for the transition parameters. In addition the theory predicts the existence of limiting densities for the two phases; the numerical values calculated for these limiting densities are in very good agreement with the dense random close packed³ and the face-centered-crystal close packed values.

This paper reports an extension of our previously published analysis to the description of freezing in the Lennard-Jones system. We shall show that replacement of the hard sphere potential with the Lennard-Jones

potential, with the consequent softening of the repulsive interaction and addition of the attractive interaction, introduces new and qualitatively different features into the description of the system at very high densities. The work reported differs from earlier studies of freezing in the Lennard-Jones system in several respects. First, previous attempts to use bifurcation theory^{4,5} were flawed by the neglect of the change in density accompanying the phase transition, and by the replacement of the pair correlation function of the crystal by that of the coexisting liquid. These particular approximations lead to an incorrect bifurcation point, as we showed in an earlier paper.¹ Second, we are able to describe the freezing line in the temperature-density plane in terms of changes in the structures of the coexisting phases in rather more detail than is possible with other approaches.^{4,5} Third, we are led to an interesting conjecture concerning spinodal decomposition.

II. THEORETICAL BACKGROUND

A. Structure of the theory

Our approach to the theory of freezing is described in Ref. 1, to which we refer the reader for details. The analysis starts with the following exact expansion for the singlet distribution function as a function of position, $\rho(\mathbf{R}_1)$, of an inhomogeneous fluid:

$$\begin{aligned} \frac{\rho(\mathbf{R}_1)}{z} &= \exp \left[\sum_{k=1}^{\infty} \frac{1}{k!} \int S_{k+1}(\mathbf{R}_1, \dots, \mathbf{R}_{k+1}) \right. \\ &\quad \left. \times \rho(\mathbf{R}_2) \dots \rho(\mathbf{R}_{k+1}) d\mathbf{R}_2 \dots d\mathbf{R}_{k+1} \right] \\ &= \exp[F(\mathbf{R}_1, \{\rho(\mathbf{R}_i)\})], \end{aligned} \quad (1)$$

where $S_{k+1}(\mathbf{R}_1, \dots, \mathbf{R}_{k+1})$ is the sum of all irreducible Mayer cluster diagrams of order $k+1$. The fugacity, z , is determined by

$$\lim_{V \rightarrow \infty} \frac{1}{V} \int d\mathbf{R} \rho(\mathbf{R}) = \rho, \quad (2)$$

where ρ is the mean density of the system. The argument of the exponential term on the right-hand side of Eq. (1), $F(\mathbf{R}_1, \{\rho(\mathbf{R}_i)\})$, is the generating function of the n -particle direct correlation function $c_n(\mathbf{R}_1, \dots, \mathbf{R}_n)$,^{6,7}

$$c_n(\mathbf{R}_1, \dots, \mathbf{R}_n) = \frac{\delta^{n-1} F(\mathbf{R}_1, \{\rho(\mathbf{R}_i)\})}{\delta \rho(\mathbf{R}_2) \dots \delta \rho(\mathbf{R}_n)}. \quad (3)$$

^{a)} Present address: The Institute of Physical Science and Technology, The University of Maryland, College Park, Maryland, 20742.

^{b)} Present address: Lawrence Livermore Laboratory, Livermore, California 94550.

A functional Taylor expansion of this generating function about its liquid state value $F(\mathbf{R}_1, \{\rho_l\})$, truncated after the first three terms, leads to

$$\frac{\rho(\mathbf{R}_1)}{z_s} = \frac{\rho_l}{z_l} \exp \left[\int d\mathbf{R}_2 c_2(\mathbf{R}_{12}, \rho_l) \Delta\rho(\mathbf{R}_2) + \frac{1}{2} \iint d\mathbf{R}_2 d\mathbf{R}_3 c_3(\mathbf{R}_1, \mathbf{R}_2, \mathbf{R}_3; \rho_l) \Delta\rho(\mathbf{R}_2) \Delta\rho(\mathbf{R}_3) \right], \quad (4)$$

where $\Delta\rho(\mathbf{R})$ is the density difference $\rho(\mathbf{R}) - \rho_l$. In Eq. (4), ρ_s and z_s are the density and the fugacity of the solid phase, with ρ_l and z_l the analogous liquid phase quantities. In obtaining Eq. (4) the following identifications have been made:

$$F(\mathbf{R}_1, \{\rho_l\}) = \ln \left(\frac{\rho_l}{z_l} \right), \quad (5a)$$

$$F(\mathbf{R}_1, \{\rho(\mathbf{R}_i)\}) = \ln \left(\frac{\rho_s}{z_s} \right), \quad (5b)$$

$$c_2(\mathbf{R}_1, \mathbf{R}_2; \rho_l) = c_2(\mathbf{R}_{12}, \rho_l). \quad (5c)$$

In order that the role of the crystal structure be made explicit, the singlet density distribution function for the crystalline phase is expanded in a Fourier series,

$$\begin{aligned} \rho(\mathbf{R}) &= \rho_l + \Delta\rho(\mathbf{R}) \\ &= \rho_l(1 + \phi_0) + \rho_l \sum_{\mathbf{G}} \phi_{\mathbf{G}} \exp(i\mathbf{G} \cdot \mathbf{R}), \end{aligned} \quad (6)$$

where the $\{\mathbf{G}\}$ are the reciprocal lattice vectors of the crystal and the $\phi_{\mathbf{G}}$ are the expansion coefficients

$$\phi_{\mathbf{G}} = \frac{1}{\Delta} \int_{\Delta} \frac{\Delta\rho(\mathbf{R})}{\rho_l} \exp(-i\mathbf{G} \cdot \mathbf{R}) d\mathbf{R}, \quad (7)$$

with Δ the volume of a unit cell. Clearly, ϕ_0 is the fractional density difference between the liquid and solid phases. Equation (6) is now combined with Eq. (4) to yield

$$\begin{aligned} \frac{\rho(\mathbf{R}_1)}{z_s} &= \frac{\rho_l}{z_l} \exp \left[\rho_l \phi_0 \bar{c}_2(0) + \rho_l \sum_{\mathbf{G}} \phi_{\mathbf{G}} \bar{c}_2(\mathbf{G}) \exp(i\mathbf{G} \cdot \mathbf{R}_1) + \frac{1}{2} \rho_l^2 \phi_0^2 \bar{c}_3(0, 0) + \rho_l^2 \phi_0 \sum_{\mathbf{G}} \phi_{\mathbf{G}} \bar{c}_3(\mathbf{G}, 0) \exp(i\mathbf{G} \cdot \mathbf{R}_1) \right. \\ &\quad \left. + \frac{1}{2} \rho_l^2 \sum_{\mathbf{G}, \mathbf{G}'} \phi_{\mathbf{G}} \phi_{\mathbf{G}'} \bar{c}_3(\mathbf{G}, \mathbf{G}') \exp[i(\mathbf{G} + \mathbf{G}') \cdot \mathbf{R}_1] \right], \end{aligned} \quad (8)$$

where

$$\bar{c}_2(\mathbf{G}) = \int d\mathbf{R}_{12} \exp(i\mathbf{G} \cdot \mathbf{R}_{12}) c_2(\mathbf{R}_{12}, \rho_l), \quad (9a)$$

$$\bar{c}_3(\mathbf{G}, \mathbf{G}') = \int d\mathbf{R}_{12} \int d\mathbf{R}_{13} \exp(i\mathbf{G} \cdot \mathbf{R}_{12} + i\mathbf{G}' \cdot \mathbf{R}_{13}) c_3(\mathbf{R}_1, \mathbf{R}_2, \mathbf{R}_3; \rho_l). \quad (9b)$$

For technical reasons it is convenient to remove the fugacities z_l and z_s from Eq. (8) by following the procedure described earlier.^{1,2} The method consists of forming n independent equations by using the orthogonality properties of the Fourier series in Eq. (6) and then removing the fugacities by dividing out the first relationship. The resulting expression is

$$\begin{aligned} &\left(\frac{\rho_l}{\rho_s} \right) \Delta_{\mathbf{G}_\alpha} \phi_{\mathbf{G}_\alpha} \\ &= \frac{\int d\mathbf{R}_1 \xi_{\mathbf{G}_\alpha}(\mathbf{R}_1) \exp \left[\rho_l \sum_{\mathbf{G}} \phi_{\mathbf{G}} \bar{c}_2(\mathbf{G}) \xi_{\mathbf{G}}(\mathbf{R}_1) + \rho_l^2 \phi_0 \sum_{\mathbf{G}} \phi_{\mathbf{G}} \bar{c}_3(\mathbf{G}, 0) \xi_{\mathbf{G}}(\mathbf{R}_1) + \frac{1}{2} \rho_l^2 \sum_{\mathbf{G}, \mathbf{G}'} \phi_{\mathbf{G}} \phi_{\mathbf{G}'} \bar{c}_3(\mathbf{G}, \mathbf{G}') \xi_{\mathbf{G}+\mathbf{G}'}(\mathbf{R}_1) \right]}{\int d\mathbf{R}_1 \exp \left[\rho_l \sum_{\mathbf{G}} \phi_{\mathbf{G}} \bar{c}_2(\mathbf{G}) \xi_{\mathbf{G}}(\mathbf{R}_1) + \rho_l^2 \phi_0 \sum_{\mathbf{G}} \phi_{\mathbf{G}} \bar{c}_3(\mathbf{G}, 0) \xi_{\mathbf{G}}(\mathbf{R}_1) + \frac{1}{2} \rho_l^2 \sum_{\mathbf{G}, \mathbf{G}'} \phi_{\mathbf{G}} \phi_{\mathbf{G}'} \bar{c}_3(\mathbf{G}, \mathbf{G}') \xi_{\mathbf{G}+\mathbf{G}'}(\mathbf{R}_1) \right]}, \end{aligned} \quad (10)$$

with

$$\xi_{\mathbf{G}_\alpha}(\mathbf{R}_1) = \sum_j \exp(i\mathbf{G}_{j\alpha} \cdot \mathbf{R}_1), \quad (11a)$$

$$\Delta_{\mathbf{G}_\alpha} = \frac{1}{\Delta} \int d\mathbf{R} \xi_{\mathbf{G}_\alpha}^2(\mathbf{R}_1). \quad (11b)$$

$\phi_{\mathbf{G}_\alpha}$ is the order parameter of the α th reciprocal lattice vector.

Equation (10) defines a system of nonlinear equations which is conveniently reduced to parametric form by neglecting the triplet correlation terms $\bar{c}_3(\mathbf{G}, 0)$ and $\bar{c}_3(\mathbf{G}, \mathbf{G}')$ and introducing the variables $\psi_{\mathbf{G}_\alpha}$ and $\lambda_{\mathbf{G}_\alpha}$ defined by

$$\frac{\rho_l}{\rho_s} \phi_{\mathbf{G}_\alpha} \equiv \psi_{\mathbf{G}_\alpha} \quad (12a)$$

and

$$\rho_s \bar{c}_2(\mathbf{G}_\alpha) \equiv \lambda_{\mathbf{G}_\alpha}. \quad (12b)$$

This procedure generates the closed system of equations

$$\psi_{\mathbf{G}_\alpha} = \frac{\int d\mathbf{R}_1 \xi_{\mathbf{G}_\alpha}(\mathbf{R}_1) \exp \left[\sum_{\mathbf{G}} \psi_{\mathbf{G}} \lambda_{\mathbf{G}} \xi_{\mathbf{G}}(\mathbf{R}_1) \right]}{\int d\mathbf{R}_1 \exp \left[\sum_{\mathbf{G}} \psi_{\mathbf{G}} \lambda_{\mathbf{G}} \xi_{\mathbf{G}}(\mathbf{R}_1) \right]}. \quad (13)$$

Equation (13) can be solved for the bifurcation points directly without using any information about the liquid state correlation functions. Thus, the bifurcation diagram generated by Eq. (13) is "universal" for a chosen lattice.

Calculations by Ramakrishnan and Yussouff,^{8,9,10} and by Haymet and Oxtoby¹¹ indicate that, for some systems, neglect of the triplet correlation functions can lead to serious errors. In the next level of approximation, the truncated form of Eq. (10) keeps $\tilde{c}_3(\mathbf{G}, 0)$ and neglects $\tilde{c}_3(\mathbf{G}, \mathbf{G}')$. Then, if we use, instead of Eq. (12b), the parametrization

$$\rho_s [\tilde{c}_2(\mathbf{G}_\alpha) + \rho_l \phi_0 \tilde{c}_3(\mathbf{G}_\alpha, 0)] = \lambda_{\mathbf{G}_\alpha}, \quad (12c)$$

the form of Eq. (13) is preserved and hence the bifurcation analysis remains unaltered. It must be noted that we know nothing about the relative importance of the terms $\tilde{c}_3(\mathbf{G}, 0)$ and $\tilde{c}_3(\mathbf{G}, \mathbf{G}')$, so the approximation generated by retaining one and neglecting the other is uncontrolled. However, as shown by Ramakrishnan and Yussouff and confirmed by Haymet,¹² retention of $\tilde{c}_3(\mathbf{G}, 0)$ and neglect of $\tilde{c}_3(\mathbf{G}, \mathbf{G}')$ does improve the numerical accuracy of the predicted properties of the freezing transition.

In the calculation reported in this paper we have terminated the Fourier expansion in Eq. (6) after two order parameter sets. The resulting theory is referred to as a two order parameter theory. The accuracy of predictions can be improved by inclusion of higher order parameter sets. However, the predictions obtained from the similar theory of Ramakrishnan and Yussouff⁸ differ by only 5% with and without the inclusion of these higher order terms, so that for many purposes a two order parameter theory should suffice.

B. Bifurcation analysis

Since the Lennard-Jones fluid preferentially freezes into a face-centered-cubic (fcc) lattice, we consider only this geometry. The first and second reciprocal lattice vector sets of the fcc lattice are

$$\xi_{\mathbf{G}_\alpha}(\mathbf{R}) = 8 \cos\left(\frac{2\pi}{a}x\right) \cos\left(\frac{2\pi}{a}y\right) \cos\left(\frac{2\pi}{a}z\right) \quad (14)$$

and

$$\begin{aligned} \xi_{\mathbf{G}_\beta}(\mathbf{R}) = & 8 \cos\left(\frac{6\pi}{a}x\right) \cos\left(\frac{2\pi}{a}y\right) \cos\left(\frac{2\pi}{a}z\right) \\ & + 8 \cos\left(\frac{2\pi}{a}x\right) \cos\left(\frac{6\pi}{a}y\right) \cos\left(\frac{2\pi}{a}z\right) \\ & + 8 \cos\left(\frac{2\pi}{a}x\right) \cos\left(\frac{2\pi}{a}y\right) \cos\left(\frac{6\pi}{a}z\right), \end{aligned} \quad (15)$$

with

$$\Delta = a^3 = 4\rho_s^{-1}, \quad \Delta_{\mathbf{G}_\alpha} = 8, \quad \Delta_{\mathbf{G}_\beta} = 24, \\ |\mathbf{G}_\alpha| = 2\pi\sqrt{3}(\rho_s/4)^{1/3}, \quad |\mathbf{G}_\beta| = 2\pi\sqrt{11}(\rho_s/4)^{1/3}, \quad (16)$$

where a is the nearest neighbor spacing in the crystal. Using these expressions, the coupled nonlinear integral equations for the two order parameters assume the forms¹

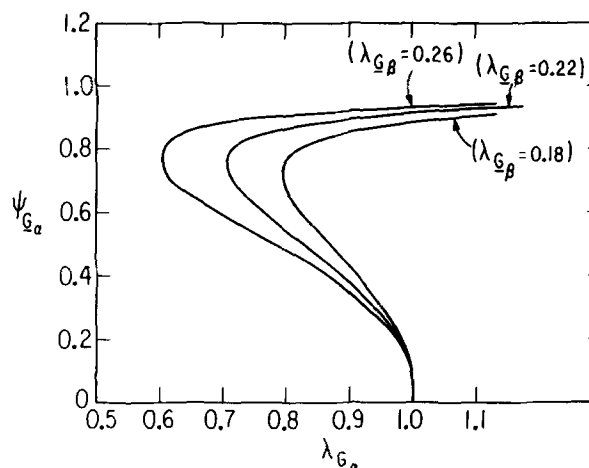


FIG. 1. Two order parameter bifurcation curves for the fcc lattice for different values of $\lambda_{\mathbf{G}_\beta}$.

$$8\psi_{\mathbf{G}_\alpha} = \frac{\int_{\Delta} d\mathbf{R}_1 \xi_{\mathbf{G}_\alpha}(\mathbf{R}_1) \exp[\psi_{\mathbf{G}_\alpha} \lambda_{\mathbf{G}_\alpha} \xi_{\mathbf{G}_\alpha}(\mathbf{R}_1) + \psi_{\mathbf{G}_\beta} \lambda_{\mathbf{G}_\beta} \xi_{\mathbf{G}_\beta}(\mathbf{R}_1)]}{\int_{\Delta} d\mathbf{R}_1 \exp[\psi_{\mathbf{G}_\alpha} \lambda_{\mathbf{G}_\alpha} \xi_{\mathbf{G}_\alpha}(\mathbf{R}_1) + \psi_{\mathbf{G}_\beta} \lambda_{\mathbf{G}_\beta} \xi_{\mathbf{G}_\beta}(\mathbf{R}_1)]}, \quad (17)$$

and

$$24\psi_{\mathbf{G}_\beta} = \frac{\int_{\Delta} d\mathbf{R}_1 \xi_{\mathbf{G}_\beta}(\mathbf{R}_1) \exp[\psi_{\mathbf{G}_\alpha} \lambda_{\mathbf{G}_\alpha} \xi_{\mathbf{G}_\alpha}(\mathbf{R}_1) + \psi_{\mathbf{G}_\beta} \lambda_{\mathbf{G}_\beta} \xi_{\mathbf{G}_\beta}(\mathbf{R}_1)]}{\int_{\Delta} d\mathbf{R}_1 \exp[\psi_{\mathbf{G}_\alpha} \lambda_{\mathbf{G}_\alpha} \xi_{\mathbf{G}_\alpha}(\mathbf{R}_1) + \psi_{\mathbf{G}_\beta} \lambda_{\mathbf{G}_\beta} \xi_{\mathbf{G}_\beta}(\mathbf{R}_1)]}. \quad (18)$$

It is possible to find a solution for the simultaneous Eqs. (17) and (18) by finding a relationship between $\lambda_{\mathbf{G}_\alpha}$ and $\lambda_{\mathbf{G}_\beta}$; this relationship is obtained by fixing $\lambda_{\mathbf{G}_\beta}$ and searching for bifurcation points as a function of $\lambda_{\mathbf{G}_\alpha}$. In this fashion bifurcation diagrams such as that shown in Fig. 1 can be generated. The details of the numerical procedure and the physical significance of the different features of the bifurcation diagram are discussed in Ref. 1. A discussion relevant to the present study will be given in Sec. III.

C. Density computations

By solving the simultaneous nonlinear integral Eqs. (17) and (18) for the bifurcation points, a "universal" bifurcation curve, as shown in Fig. 2, can be constructed. The curve is approximately linear for large values of $\lambda_{\mathbf{G}_\beta}$, but deviates from linearity as $\lambda_{\mathbf{G}_\beta}$ approaches zero. No information about $\tilde{c}_2(\mathbf{G})$ is used to construct the line of bifurcations shown in Fig. 2.

The liquid and solid phase transition densities can be calculated as follows. For any fixed temperature there can be only one point on the bifurcation line which corresponds to the transition densities. This point is found by solving the following system of equations:

$$\lambda_{\mathbf{G}_\alpha}(\rho_l^*, \rho_s^*) = \lambda_{\mathbf{G}_\alpha}^*, \quad (19)$$

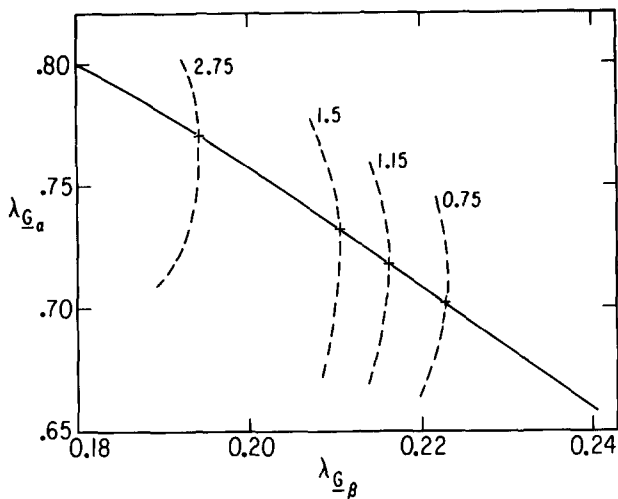


FIG. 2. The bifurcation line generated by the fcc system. The solid line indicates the functional relationship of the bifurcation points; the broken lines display the self-consistent solution search at different temperatures. The temperatures are indicated on the graph.

$$\frac{\partial}{\partial \rho_s} \lambda_{G\alpha}(\rho_i^*, \rho_s^*) = 0, \quad (20)$$

$$\lambda_{G\beta}(\rho_i^*, \rho_s^*) = \lambda_{G\beta}^*, \quad (21)$$

where (ρ_i^*, ρ_s^*) are the transition densities and $(\lambda_{G\alpha}^*, \lambda_{G\beta}^*)$ is a pair of values on the bifurcation line.

It is worthwhile to discuss briefly the significance of the condition expressed as Eq. (20). This equation represents a structural condition arising from the existence of a sharp maximum in the direct correlation function for the liquid near $|\mathbf{G}_\alpha|$, the magnitude of the first reciprocal lattice vector, and from the monotonic dependence of the maximum of $\lambda_{G\alpha}$ on the liquid density (Fig. 3). Put in a different way, this condition, along with conditions (19) and (21), guarantees that the densities predicted by the solutions to the nonlinear equations are the lowest for which the liquid becomes unstable relative to the fcc crystal as the liquid density is increased. Since Eq. (20) is independent of Eqs. (17) and (18), the solution of the pair of simultaneous Eqs. (19) and (20) will lie on a different line than the bifurcation line. The intersection of this line with the bifurcation line yields the characteristic properties of the liquid and solid phases in equilibrium along the freezing line.

In order to solve Eqs. (19)–(21), an expression for the direct correlation function of the liquid is required. In the treatment of freezing of the hard sphere fluid given in Ref. 1, we used the Wertheim–Thiele solution¹³ of the Percus–Yevick equation.¹⁴ Fortunately, the Percus–Yevick approximation to the direct correlation function is very accurate in Fourier space,¹⁵ and in particular near the first peak of $\tilde{c}_2(G)$, which peak has considerable influence on the accuracy of solution of Eq. (20). Although the Percus–Yevick direct correlation function is somewhat shifted from the function determined by computer simulations near the second peak of $\tilde{c}_2(G)$ and beyond, inclusion of corrections,

such as those proposed by Verlet and Weis,¹⁶ do not lead to any significant change in the results of the analysis.

For the case of the Lennard-Jones fluid, discussed in this paper, we have used the perturbation theory of Weeks, Chandler, and Andersen (WCA)¹⁶ to compute the structure factor $S(k)$, hence the direct correlation function. In the WCA theory the Fourier transform, $\tilde{h}(k)$, of the pair correlation function, $h(R)$, is given by

$$\tilde{h}(k) = \tilde{h}_d(k) + \int d\mathbf{R} y_d(\mathbf{R}) \times \{ \exp[-\beta u_0(R)] - \exp[-\beta u_d(R)] \} \exp(-i\mathbf{k} \cdot \mathbf{R}), \quad (22)$$

where $\tilde{h}_d(k)$ is the Fourier transform of the pair correlation function of a system of hard spheres with a well-defined temperature and density dependent hard core diameter, $u_d(R)$ is the hard-sphere interaction potential, and $u_0(R)$ is given by

$$u_0(R) = u_{LJ}(R) + 1; \quad R < 2^{1/6}\sigma, \\ = 0; \quad R \geq 2^{1/6}\sigma, \quad (23)$$

with $u_{LJ}(r)$ the 6-12 Lennard-Jones potential

$$\mu_{LJ}(R) = 4\epsilon \left[\left(\frac{\sigma}{R} \right)^{12} - \left(\frac{\sigma}{R} \right)^6 \right]. \quad (24)$$

Finally, the function $y_d(r)$ is given approximately by the following:

$$y_d(R) = -c_2(R); \quad R < d, \\ = h_d(R) + 1; \quad R > d. \quad (25)$$

For the temperature and density dependence of the hard sphere diameter we have used the expressions provided by Verlet and Weis,¹⁵ together with their correction term for $h(r)$. The direct correlation function is then computed from $\tilde{h}(k)$ using the Fourier space definition

$$\tilde{c}_2(k) \equiv \frac{\tilde{h}(k)}{1 + \rho_l \tilde{h}(k)}. \quad (26)$$

The $\tilde{c}_2(k)$ thus obtained may then be used to solve Eqs. (19)–(21) to evaluate the liquid and crystal densities

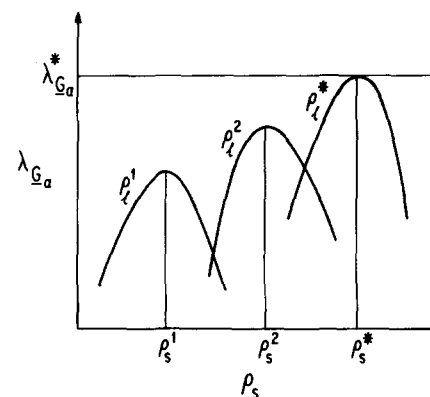


FIG. 3. The monotonic behavior of $\lambda_{G\alpha}$ as a function of solid density (ρ_s) for several values of liquid density (ρ_l). The first intersection of the curve with the constant $\lambda_{G\alpha}^*$ yields the transition densities.

TABLE I. Numerical values of freezing parameter for Lennard-Jones fcc transition.

Temperature T^*	$\lambda_{G_\alpha}^*$	$\lambda_{G_\beta}^*$	ρ_l^*	ρ_s^*	ϕ_0
0.75	0.702	0.223	0.807	0.995	0.232
Expt.	0.83-0.85	0.93-0.95	0.12
1.15	0.7183	0.216	0.846	1.0537	0.245
Expt.	0.90-0.92	0.98-1.0	0.10
1.35	0.725	0.214	0.865	1.081	0.25
Expt.	0.91-0.93	1.0-1.02	0.098
2.74	0.77	0.194	0.994	1.242	0.249
Expt.	1.06-1.08	1.13-1.15	0.07

along the transition line.

It is well known¹⁴ that the WCA approximation yields a very accurate prediction of the pair correlation function of a Lennard-Jones fluid near the triple point, but that the approximation worsens as one moves away from the triple point by varying either the temperature or density. It is also known that the WCA approximation is more accurate in Fourier space the larger the value of the wave vector, since the assumptions of the theory are best satisfied for $k > \pi/\sigma$. In our calculation the direct correlation function is needed for values of k much larger than π/σ , so the WCA approximation should provide a reliable description of $\tilde{c}_2(k)$ over a considerable range of temperature and density, provided that the density of the liquid remains sufficiently large ($\rho_l > 0.6$). This condition is always satisfied in the calculations presented in this paper.

The dashed lines in Fig. 2 show the solution of Eqs. (19)–(21) for several temperatures. The values of the liquid and crystal densities are compared along the transition line with the computer simulation results in Table I. The predicted densities are in fairly good agreement with the computer simulation results.^{14,17} Note that the predicted densities for both the liquid and solid phases along the freezing line decrease linearly with decreasing temperature (see Fig. 4) as do the densities found by computer simulations.^{14,17} However, there is a large discrepancy between the theoretical and observed fractional density changes ϕ_0 . The predicted fractional density change on freezing remains constant as a function of temperature, which is not in agreement with the computer simulation data. Furthermore, the predicted fractional density change on freezing is too large, an error similar to that found in the Bagchi, Cerjan, and Rice¹ theory of freezing of a hard sphere fluid.

IV. DISCUSSION

In our earlier study of freezing of a hard sphere fluid to a face centered cubic crystal we found that the system of non linear integral equations used to describe the transition displays two bifurcation points. One of these we identified with the freezing transition; for the hard sphere fluid this transition occurs when the fluid density has a specific value, and is not at all dependent on the temperature of the system. The second

bifurcation point was found to be universal in the sense that it arises solely from the structure of the equations; it was identified with the achievement of the limits of closest packing for the fluid and crystal phases. The numerical values predicted for the random closest packing of the fluid, and the closest packing of the fcc lattice, agree with the known values.

Our study of the freezing of a Lennard-Jones fluid to a face-centered-cubic crystal also leads to the conclusion that the system of nonlinear integral equations used to describe the transition displays two bifurcation points. One of these we associate with the freezing transition, as described in the last section. Moreover, for the Lennard-Jones fluid this bifurcation point changes as the fluid density changes. The line of bifurcations that is so generated is then used to calculate the freezing line in the density-temperature plane. And, just as for the hard sphere fluid, the second bifurcation point is universal in the sense that it arises solely from the structure of the equations. But, unlike the hard sphere fluid, there is no limit of closest packing in a system composed of particles that have a soft repulsive interaction. Does the second bifurcation point for the inhomogeneous density distribution in a Lennard-Jones fluid signal a real phenomenon or is it an artifact of the approximations used in our analysis? We shall conjecture an answer to this question below.

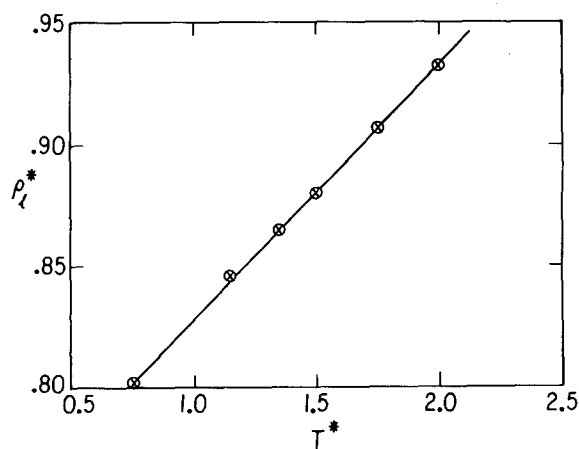


FIG. 4. The linear dependence of the calculated liquid transition density on the temperature of the system.

First, however, consider the properties of the liquid and crystal phases along the freezing line predicted from our theory. We have already pointed out, in the last section, the nature of the discrepancies between predicted and observed properties along the freezing line. Just as for the theory of freezing of the hard sphere fluid, we attribute these discrepancies to the following sources: (a) The neglect of the wave vector dependence of the three particle direct correlation function and the complete omission of the contributions from all higher order direct correlation functions leads to an incomplete description of the ordering in the liquid phase. It is likely, but not certain, that the net effect of these omissions is to overestimate the entropy of the liquid phase, thereby artificially extending its domain of stability. (b) The approximate two particle direct correlation function we have used, although apparently accurate for wave vectors $k > \pi/\sigma$, is likely inaccurate to different extents for different densities, i. e., the WCA approximation likely gives less accurate derivatives of $\tilde{c}_2(k)$ than the estimate of the function itself. The density and temperature derivatives of $\tilde{c}_2(k)$ are related to the three and four particle distribution functions. Since the signs of the errors made in the implied three and four particle distribution functions are not known little can be said about their influence on our predictions. (c) The neglect of vibrational motion in the solid leads to an underestimate of the entropy of that phase. This observation, together with that of (a) concerning the entropy of the fluid, implies that the predicted entropy change on freezing will be too large, as we find. (d) The truncation of the order parameter expansion of the density difference between the liquid and solid phases leads to an overestimate of the entropy of the crystal, and to a lack of discrimination between possible structures that have the same retained reciprocal lattice vectors but differ in the other higher order reciprocal lattice vectors. Although this error in the entropy of the crystal is of opposite sign to that discussed in (c), the magnitudes of the two errors are unknown, so the balance between them is also unknown.

If we accept that the functional identification of the bifurcation point with the freezing point is valid, and that the errors arise from the approximations described above, we can improve the numerical predictions of the theory by eliminating the spurious over or underestimates of the entropies of the two phases. Had we not made any approximations, the chemical potentials of each of the phases would have been properly computed and, given that the bifurcation point coincides with the point at which the chemical potentials of the two phases are equal, the changes in thermodynamic properties across the phase transition would also have been properly computed. Because our approximations are different for the liquid and crystal, and have different effects on their chemical potentials, the bifurcation point is displaced from the point at which the approximate chemical potentials of the two phases become equal. To eliminate the net effect on the location of the freezing transition due to the separate approximations used in the descriptions of the liquid and crystal we can directly impose, as a condition, the equality of chemical poten-

TABLE II. Numerical values of freezing parameters for Lennard-Jones fcc transition with thermodynamic constraint added.

T^*	$\lambda_{G_\alpha}^*$	$\lambda_{G_\beta}^*$	ρ_l^*	ρ_s^*	ϕ_0
0.75	0.728	0.270	0.907	0.963	0.062
1.15	0.726	0.266	0.957	1.011	0.056
1.35	0.728	0.270	0.973	1.032	0.060
2.75	0.728	0.272	1.076	1.142	0.061

tials. Ramakrishnan and Yussouff^{8,9,10} and Haymet and Oxtoby¹¹ have shown that, for a description of the liquid and crystal such as we use, this condition takes the form

$$0 = (\rho_l c_0 - 1)\phi_0 + \frac{1}{2}c_0\rho_l\phi_0^2 + \frac{1}{2}\rho_l \sum_{\alpha} \tilde{c}_2(G_\alpha)\phi_{G_\alpha}^2, \quad (27)$$

where $c_0 \equiv \tilde{c}_2(0)$. The results obtained by use of Eq. (27), with the WCA approximation for c_0 , are shown in Table II. As expected, and as found in the parallel description of the freezing transition in the hard sphere system, the agreement between calculations and observations is considerably improved relative to that obtained from the original bifurcation analysis.

We now turn to the interpretation of the physical implications of the universal bifurcation point $\lambda_{G_\alpha} = 1$. As already noted, in the hard sphere system this bifurcation point represents achievement, simultaneously, of the limits of closest packing for the fluid and the face-centered-cubic lattice. There is no physical solution to the equation for the inhomogeneous density distribution of the system for any higher density, as should be the case given the physical meaning of closest packing. Note that an ordinary thermodynamic path, say one that starts in the pure fluid and proceeds via states of increasing density, cannot reach these limits since the freezing transition occurs before the density of closest packing of the fluid is reached. In terms of our analysis, the bifurcation of the solution to the equation for the inhomogeneous density distribution of the system which represents freezing always occurs at lower density than the one which represents reaching the closest packing density. For all densities higher than the freezing density the liquid branch of the density distribution has higher chemical potential than does the face centered cubic lattice branch.¹⁸ It is possible, in principle, for other bifurcation points to lie between that corresponding to the freezing transition and that corresponding to closest packing of the fluid and face centered cubic phases. We shall describe elsewhere the results of our search for such bifurcation points.¹⁹

In our interpretation the bifurcation point at $\lambda_{G_\alpha} = 1$ for the hard sphere system is not one at which the system becomes unstable, although no fluid solution exists for densities higher than that corresponding to this point. Nevertheless, we conjecture that the bifurcation point at $\lambda_{G_\alpha} = 1$ for the Lennard-Jones fluid corresponds to the spinodal for that temperature. That is, we regard the lack of fluid solutions for densities

TABLE III. Values of liquid and crystal densities for $\lambda_{G\alpha}=1$.

T^*	ρ_l^*	ρ_s^*
0.20	1.05	1.20
0.44	1.10	1.26
0.50	1.11	1.27
0.75	1.16	1.32
1.05	1.20	1.38
1.15	1.21	1.39
1.35	1.24	1.42
2.75	1.36	1.57

greater than that corresponding to the bifurcation point at $\lambda_{G\alpha}=1$ to indicate that the fluid is absolutely unstable with respect to the face-centered-cubic lattice for such densities. We again remark that a normal thermodynamic path is interrupted by the freezing transition before $\lambda_{G\alpha}=1$ is reached, and that the fluid branch of the solution for the inhomogeneous density of the system for densities higher than that corresponding to this point has higher chemical potential than does the face-centered-cubic crystal. We display in Table III the reduced densities of the liquid and solid phases when $\lambda_{G\alpha}=1$, as a function of reduced temperature. It is interesting to note that no solution to the equations for the inhomogeneous density distribution can be found if the reduced density of the liquid is less than 1.0. Finally, just as in the case of the hard sphere fluid, it is possible in principle that for the Lennard-Jones fluid there are additional bifurcation points between that corresponding to freezing and that we have conjectured corresponds to spinodal decomposition. We shall describe elsewhere the results of our search for such bifurcation points.¹⁹

ACKNOWLEDGMENT

This research was supported by a grant from the National Science Foundation.

- ¹B. Bagchi, C. Cerjan, and S. A. Rice, *J. Chem. Phys.* (in press).
- ²V. N. Ryzhov and E. F. Tareeva, *Theor. Math. Phys.* (Moscow) **48**, 835 (1981).
- ³J. D. Bernal, *Nature (London)* **183**, 141 (1959); J. L. Finney, *Proc. R. Soc. London Ser. A* **139**, 479 (1970); D. J. Adams, and A. J. Matheson, *J. Chem. Phys.* **56**, 1989 (1972); S. Hudson and H. C. Andersen, *ibid.* **69**, 2323 (1978).
- ⁴J. G. Kirkwood and E. Monroe, *J. Chem. Phys.* **9**, 514 (1941); L. Feijo and A. Rahman, *ibid.* **77**, 5687 (1982).
- ⁵H. J. Raveche and R. F. Kayser, Jr., *J. Chem. Phys.* **68**, 3632 (1978); J. J. Kozak, S. A. Rice, and J. D. Weeks, *Physica (Utrecht)* **54**, 573 (1971); J. D. Weeks, S. A. Rice, and J. J. Kozak, *J. Chem. Phys.* **52**, 2416 (1970).
- ⁶E. A. Arinshtein, *Dokl. Akad. Nauk SSSR* **112**, 615 (1957); F. H. Stillinger and F. P. Bruff, *J. Chem. Phys.* **37**, 1 (1962).
- ⁷R. Lovett, *J. Chem. Phys.* **66**, 1225 (1977); R. Lovett and F. P. Buff, *ibid.* **72**, 2425 (1980).
- ⁸T. V. Ramakrishnan and M. Yussouff, *Phys. Rev. B* **19**, 2775 (1979); *Solid State Commun.* **21**, 389 (1977).
- ⁹M. Yussouff, *Phys. Rev. B* **23**, 5871 (1981).
- ¹⁰T. V. Ramakrishnan, *Phys. Rev. Lett.* **48**, 541 (1982).
- ¹¹A. D. J. Haymet and D. W. Oxtoby, *J. Chem. Phys.* **74**, 2559 (1981).
- ¹²A. D. J. Haymet, *J. Chem. Phys.* **78**, 4641 (1983).
- ¹³M. S. Wertheim, *Phys. Rev. Lett.* **10**, 321 (1963); E. Thiele, *J. Chem. Phys.* **39**, 474 (1963); M. S. Wertheim, *J. Math. Phys.* **5**, 643 (1964).
- ¹⁴J. P. Hansen and J. R. McDonald, *Theory of Simple Liquids* (Academic, London, 1976).
- ¹⁵L. Verlet and J. J. Weis, *Phys. Rev. A* **5**, 939 (1972).
- ¹⁶J. D. Weeks, D. Chandler, and H. C. Andersen, *J. Chem. Phys.* **54**, 5237 (1971).
- ¹⁷W. B. Street, H. J. Raveche, and R. D. Mountian, *J. Chem. Phys.* **61**, 1980 (1974).
- ¹⁸C. Cerjan and B. Bagchi, *Phys. Rev. B* (in press).
- ¹⁹B. Bagchi, C. Cerjan, and S. A. Rice (in preparation).